Liquid Crystal Polymer-Based Planar Lumped Component Dual-Band Filters For Dual-Band WLAN Systems[1]

Amit Bavisi[1], Madhavan Swaminathan[2], and Essam Mina[1]

[1] IBM, Systems and Technology Group, 1000 River Street, Essex Junction, VT 05495
[2] School of Electrical and Computer Engineering, Georgia Institute of Technology, Atlanta, Ga 30332

ABSTRACT — **This paper presents the design and implementation of dual-band filters using lumped components that are completely embedded in a multi-layer organic process technology, which incorporates multiple liquid crystalline polymer (LCP) substrates. The paper presents the design methodology and measurement results of the small form factor fully-integrated filters that are directly applicable to WLAN systems. The fully-functional embodiments of single-input single-output filters were designed to have passbands with independently controllable bandwidths around the center frequencies of 2.4 GHz and 5.2 GHz. The filters present low insertion loss (~1.1 dB) and return loss better than 15 dB at both the frequencies. The fully-packaged filters were designed in an area of 5.1 x 5.3 mm2, providing a 5X reduction in area as compared to any previously reported works on dual-band filters.**

Index Terms — **Dual-band filters, bandpass filters, LCP, WLAN, dual-band.**

I. INTRODUCTION

Over the past few years, wireless networking (WLAN) has captured the imagination of both cellular and notebook consumers worldwide, and has emerged as one of the fastest growing semiconductor markets. For instance, in 2002 WLAN chipset market was approximately $400 million and is forecasted to be over $2.2 billion by the year 2007 [1]. Portable network interface cards (NICs) for WLAN, like cellular handsets, follow the trend of miniaturization with maximum integrated functionality. For WLAN systems these requirements map to integrating the low-speed 2.4 GHz WLAN protocol (IEEE standard 802.11b) with the high-speed 802.11g and 802.11a (5 GHz) standards in a standard PCMCIA card. The trend in system miniaturization and reduction in bill of materials (BOM) has forced WLAN system designers to incorporate frequency-agile components, tuned components, and components with multi-band characteristics. Hence, a dual-band filter with single-input and single-output is investigated in this paper. An integrated dual-band filter will result in cost reduction and reduction of module size due to reduction in (1) number of filters and (2) matching networks.

Several authors [2]-[4] have investigated dual passband characteristics in filters via the use of planar transmission lines and stepped impedances. However, the size of these planar filters is significantly large (*120 mm^2*) because the transmission lines should be at least one-half wavelengths. It was shown in [3] that in present dual-band filters the ratio of center frequencies (f_2/f_1) cannot exceed 2.3, which barely meets the current WLAN requirements (5.5 GHz/2.45 GHz ~ 2.25). Additionally, the use of transmission lines inherently limits the bandwidth at 5 GHz center frequency (~800 MHz) [2]-[4], thereby restricting the number of channels available for use in the 5 GHz frequency band. The aforementioned issues with transmission line-based dual-band filters make their application in the small form factor commercial WLAN systems very distant. This paper provides a design methodology to obtain *fully controllable dual passband characteristics from a single-input single-output filter in size-efficient manner.*

II. DESIGN METHODOLOGY

This section discusses the design of single-input single-output dual-band filters using lumped components. The design methodology uses fourth-order asynchronous LC resonators to produce two distinct passbands with controllable bandwidths. The design builds on a capacitive-coupled second-order Chebychev filter as shown in Fig.1. The circuit finds wide applications in high

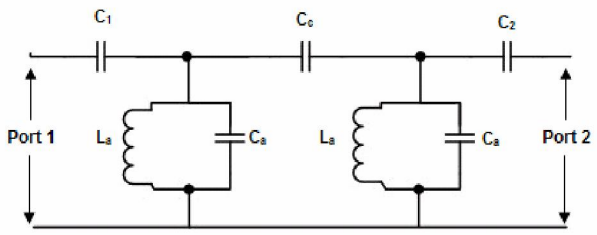

Fig.1 Single-band capacitively-coupled Chebychev filter.

[1] Patent pending

Q packaging technologies because the circuit uses more capacitive elements than inductors, which thereby reduces the losses in the filter. In Fig.1, the series capacitors C_1 and C_2 match the input and output ports of the filter to the source and load impedances. Additionally, the capacitors also finely control the passband center frequency. The coupling capacitor C_c controls the bandwidth or pass-band ripple of the filter.

Reference [5] provides the exact synthesis of the Chebychev filters. By following any of these synthesis techniques it is observed that the center frequency of the filter is governed by the values of the shunt LC resonators. Consequently, the Chebychev filter can be scaled in frequency by simply changing the value of the components L_a-C_a. Tables I and II show an example of synthesized component values for filter at 0.9 GHz and 2.4 GHz. It can be observed that the component values of the two filters differ in only their resonators. Thus, from Tables I and II it can be clearly observed that a single Chebychev filter can be used to generate two passbands by replacing the 2nd-order LC resonators with an appropriate higher order (fourth) network that can emulate series/parallel connection of multiple resonators.

(A) Design Synthesis

Fig.2 shows the schematic of the proposed lumped component-based dual-band filter. The underlying principle is to synthesize two different shunt inductors using a fourth-order resonator. The shunt inductors resonate with the input series capacitors (C_1 and C_2) at the two designed frequencies, namely 2.4 and 5.2 GHz, to produce the two passbands. The component values for the resonators are synthesized using (1) and (2). At a frequency the effective inductance (L_{eff}) of parallel connected LC resonator can be determined from the input impedance (Z_{in}) of a resonator. These were calculated as (1) and (2). Equations (1) and (2) provide the value of the inductance (L_p) and capacitance (C_p) that is required to synthesize a L_{eff} at a given frequency ω_L and C_{eff} at a given frequency ω_H, with $\omega_H > \omega_L$.

TABLE I
COMPONENT VALUES OF THE DESIGNED 2.4 GHZ FILTER

Comp-onent	$C_1 = C_2$, pF	C_c, pF	L_a, nH	C_a, pF
Values	0.6	0.22	3	1

TABLE II
COMPONENT VALUES OF THE DESIGNED 0.9 GHZ FILTER

Comp-onent	$C_1 = C_2$, pF	C_c, pF	L_a, nH	C_a, pF
Values	0.6	0.22	13	1.6

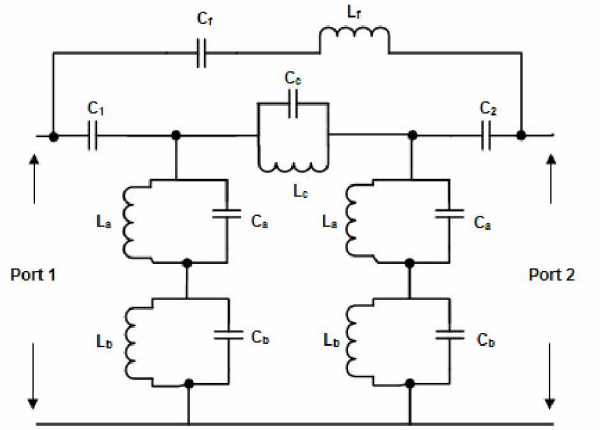

Fig.2 Proposed dual-band filter with transmission zeros.

$$L_P = L_{eff}\frac{\left(\omega_H{}^2 - \omega_L{}^2\right)}{\left(\omega_H{}^2 + \omega_H{}^2\omega_L{}^2 L_{eff} C_{eff}\right)} \quad (1)$$

$$C_P = \left(1 + \omega_H{}^2 L_P C_{eff}\right)\cdot\frac{\left(1 + \omega_L{}^2 L_{eff} C_{eff}\right)}{L_{eff}\left(\omega_H{}^2 - \omega_L{}^2\right)} \quad (2)$$

The values (L_P and C_P) obtained from expressions (1) and (2) correspond to the inductors and capacitors used in circuit simulators to obtain the desired the inductance (L_{eff}) at ω_L. The capacitive reactance at the pre-determined frequency ω_H provides a transmission zero and can be used to control the bandwidth of the lower passband. The components L_f - C_f are cross-coupling elements between the input and output providing an additional path for transmission. In effect the components function as an admittance inverter, with the admittance around the center frequency given as

$$J = Y = j\sqrt{\frac{C_f}{L_f}}\left(\frac{\omega}{\omega_0} - \frac{\omega_0}{\omega}\right) \quad (3)$$

Thus the ratio $\sqrt{L_f/C_f}$ should be close to 50 ohms to obtain a good match at both the frequencies. Additionally, the L_f-C_f components are designed to control the bandwidth of the second passband (~5 GHz). For these purposes, the value of L_f was selected to be 1.1 nH and that of C_f to be 0.6 pF. Hence, the combination provides a transmission zero at 6.2 GHz. The components L_c and C_c form a stop band filter and control the bandwidth of the lower passband by inserting a transmission zero around the lower center frequency. However, C_c also controls the insertion loss (passband ripple) of the filter [5] and hence, an optimum value of L_c needs to be selected. The remaining components were obtained via the synthesis method mentioned in [5] and then fine tuned to obtain reasonable passband characteristics, as listed in Table III.

TABLE III
DESIGNED COMPONENT VALUES FOR THE 2.4/5.2 GHZ FILTER

Component	$C_1 = C_2$, pF	C_c, pF	L_a, nH	L_b, nH	C_a, pF	C_b, pF	L_c, nH	C_f, pF	L_f, nH
Values	0.5	0.35	5	4	0.1	0.51	7.5	0.6	1.1
Qs at 2.4 GHz	308	310	83	60	-	305	65	298	-

(B) Process Technology

The filter was simulated in Sonnet™ (planar MOM full-wave solver). The eight-metal layer balanced LCP process technology was used for the design of the components. Fig.3 shows the cross-section of the balanced LCP process technology. Core 1 is a four mil thick prepreg and Core 2 is an eight mil thick prepreg. In total there are eight metal layers with the bottom-most metal layer used as a microstrip type ground reference. The configuration of the LCP and prepreg allows in a thin cross-section height (~0.75 mm) (a) passives to be distributed over different LCP layers to minimize undesired coupling, (b) large inductors can be made over the two closely spaced LCP layers, and (c) design in a stripline environment leading to minimization of losses resulting from radiation. These features make the technology especially suitable for filter design. The process supported buried-vias with 4 mils diameters and through-holes of 8 mils diameter. The combination of buried-vias and through-holes was used to achieve high component densities.

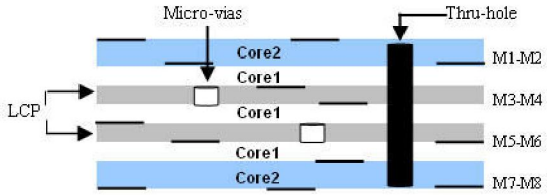

Fig.3 Cross-section of the LCP-based process technology.

Fig.4 shows the layout of the entire filter including the input-output 500 um pitch GSG probe pads. The resonators are placed on the same side of the resonator to avoid any coupling with the cross-coupling path. Microstrip interconnecting metal lines are used to physically realize the cross-coupling inductor L_f. The entire filter occupies an area of 5.1 x 5.3 mm^2.

III. EXPERIMENTAL RESULTS

The measurement to model correlation for the filter with parameters in Table III is shown in Fig.5. The filters were measured using Agilent's 8720ES vector network analyzer which was calibrated using standard SOLT techniques (1601 points, 64 averages). The effect of pads

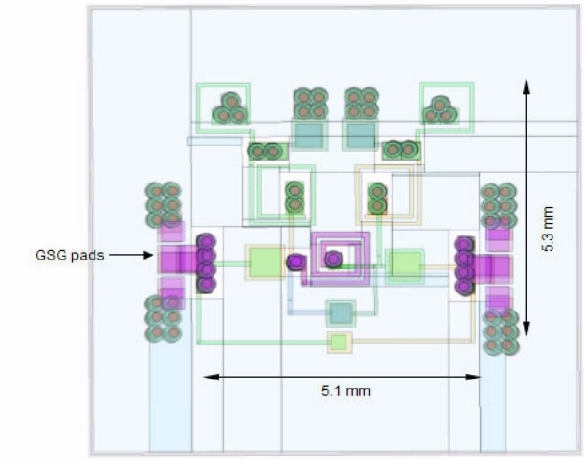

Fig.4 Layout of the designed 2.45/5.2 GHz dual-band filter.

was de-embedded from the measurements by using open calibration structures. The y-parameters of the pads were subtracted from y-parameters of the entire filter to eliminate the effect of pads (mostly capacitive) on the filter response. The pad de-embedding improved the insertion loss of the filter at both the frequency bands by approximately 0.3 dB. The transmission zero at 4.5 GHz (see Fig.5) is obtained from the change in the resonator reactance response from capacitive to inductive. An improvement in the rejection at the 4.5 GHz can be achieved by increasing the slope parameter of the resonator response *i.e.* by adding additional reactive elements in the resonator. It should be noted that the filter can achieve, at 5.2 GHz center frequency, a bandwidth

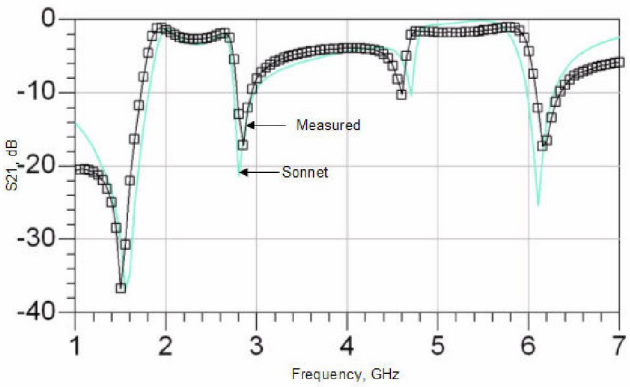

Fig.5 Model-to-hardware correlation for the 2.45/5.5 GHz dual-band filter. Sampled data: Measurement results, solid line: Sonnet simulations.

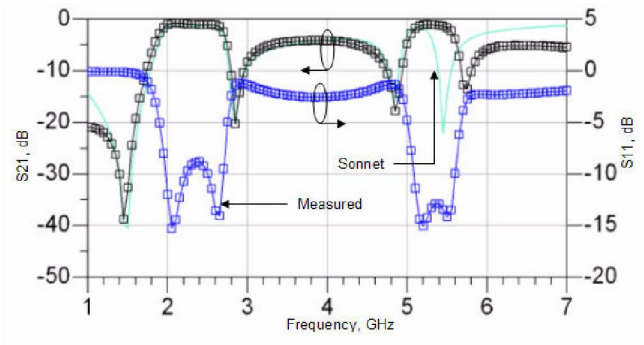

Fig.6 Model-to-hardware correlation for the 2.45/5.5 GHz dual-band filter with reduced bandwidth. The measurement shows higher bandwidth at 5 GHz than expected because of reduction in L_f.

greater than 1 GHz (~1.25 GHz) and at the same time have a smaller bandwidth at the 2.4 GHz band. The attenuation at the 3 GHz zero (see Fig.5) increases with the increase in the Q of the L_c-C_c resonant network.

Fig.6 shows the measured results of another implementation of the filter with reduced bandwidth at both the 5 GHz band. The bandwidth at 5 GHz band was reduced by increasing the value of capacitor C_f to 0.7 pF and reducing the value of inductor L_f that moved the transmission zero at 4.6 GHz from the previous design to 4.9 GHz. As a result the bandwidth at 5 GHz was reduced to 500 MHz from 1250 MHz measured previously (see Fig.5). Finally, the SRF of the capacitors C_1 and C_2 also contribute to the bandwidth at the 5.2 GHz band. Additionally, L_c was increased to 8.3 nH from 7.5 nH to reduce the bandwidth from 965 MHz to 525 MHz around the 2.4 GHz center frequency. Table IV summarizes the performance of the measured filters and compares it with other reported dual-band filters.

IV. Conclusion

This paper presented the design of dual-band filters using lumped-element components on thin multi-layered LCP substrate. The filters exhibited low insertion losses in both the frequency bands even at 6 GHz. The passband at individual frequencies can be scaled accurately and independently without requiring bulky transmission line components. The high Qs of the passive components on LCP permit low insertion losses with good out-of-band rejection characteristics without prohibitively increasing the size of the components. The design methodology coupled with broadband characteristics of passives on LCP [7] enables the separation of the two passbands (f_2/f_1) beyond 2.5, with a maximum absolute bandwidth ratio of more than 10, which is a 2.5X improvement [3] as compared to any implementation of transmission line-based filters.

The rejection between the bands can be easily increased by adding a notch filter (*e.g.* series LC network) at the filter ports.

Acknowledgement

The authors wish to acknowledge the assistance and support Mr. Charlie Russell and Mr. Venky Sundaram from Jacket Micro Devices Inc. in manufacturing support.

References

[1] Semico Research Corp., Available HTTP: http://www.semico.com/studies/category.asp?id=21, Feb. 2006.

[2] R. Bairasubramaniam, et al., "Dual-band filters for WLAN applications on LCP technology," in *IEEE Int. Microwave Symp.*, June 2005.

[3] C-M. Tsai, et al., "Planar filter design with fully controllable second passband," *IEEE Trans. Microwave Theory and Tech.*, Vol.53, pp. 3429 -3439, Nov. 2005.

[4] L-C Tsai, C-W Hsue, "Dual-band bandpass filters using equal-length coupled-serial-shunt lines and Z-transform technique," *IEEE Trans. Microwave Theory and Tech.*, vol.52, pp. 1111 - 1117, Apr. 2004.

[5] G. Matthaei, E.M.T Jones, L. Young, *Microwave Filters, Impedance-Matching Networks, and Coupling Structures,* Artech House, 1980.

[6] V. Palazzari, et al., "Design of an asymmetrical dual-band WLAN filter in LCP system-on-package technology," in *IEEE Microw. and Wireless Comp. Lett.*, Vol.15, No.3, pp. 165-167, March 2005.

[7] W. Yun, et al., "3D integration and characterization of high Q passives on multilayer LCP substrate," at *IEEE Asia Pacific Microwave Conf.*, pp. 327-330, Dec. 2005

TABLE IV
PERFORMANCE COMPARISONS OF DUAL-BAND FILTERS

References	Center frequencies, GHz	3-dB bandwidth, MHz	Insertion losses, dB	Area, mm^2
This work	2.4/5	965/1250	1.5/1.2	5.1 x 5.3
	2.4/5	525/500	1.3/1.1	5.1 x 5.3
[3]	2.4/5	NA	2.8/3.3	54 x 60
[4]	2.4/5	1000/1000	NA	125 x 30
[6]	2.4/5	NA	2.4/1.8	15 x 8